AD-A157 072 ADAPTIVE OPTICAL FILTERING TECHNIQUES(U) CALIFORNIA INST OF TECH PASADENA D PSALTIS MAY 85 RADC-TR-85-80 F30602-81-C-0169 1/1

UNCLASSIFIED F/G 20/6 NL

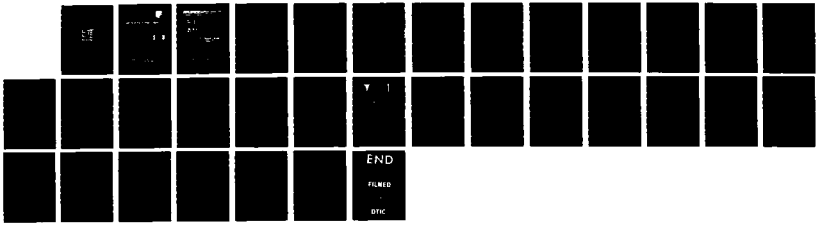

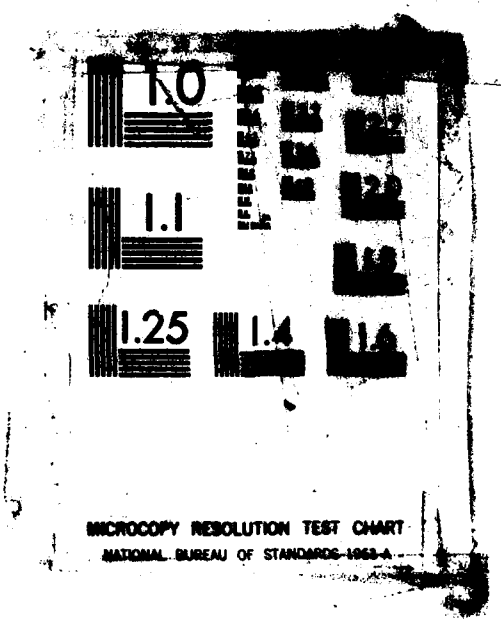
1.0
1.1
1.25
1.4
1.6
MICROCOPY RESOLUTION TEST CHART
NATIONAL BUREAU OF STANDARDS-1963-A

(2)

RADC-TR-85-80
Final Technical Report
May 1985

AD-A157 072

ADAPTIVE OPTICAL FILTERING TECHNIQUES

California Institute of Technology

Demetri Psaltis

APPROVED FOR PUBLIC RELEASE; DISTRIBUTION UNLIMITED

ROME AIR DEVELOPMENT CENTER
Air Force Systems Command
Griffiss Air Force Base, NY 13441-5700

[redacted]

If your address has changed or if you wish to be removed from the mailing list, or if the addressee is no longer employed by your organization, please notify [redacted] Griffiss AFB NY 13441-5700. This will assist us in maintaining a current mailing list.

Do not return copies of this report unless contractual obligations or notices on a specific document requires that it be returned.

UNCLASSIFIED
SECURITY CLASSIFICATION OF THIS PAGE

REPORT DOCUMENTATION PAGE

1a. REPORT SECURITY CLASSIFICATION UNCLASSIFIED	1b. RESTRICTIVE MARKINGS N/A
2a. SECURITY CLASSIFICATION AUTHORITY N/A	3. DISTRIBUTION/AVAILABILITY OF REPORT Approved for public release; distribution unlimited.
2b. DECLASSIFICATION/DOWNGRADING SCHEDULE N/A	
4. PERFORMING ORGANIZATION REPORT NUMBER(S) N/A	5. MONITORING ORGANIZATION REPORT NUMBER(S) RADC-TR-85-80
6a. NAME OF PERFORMING ORGANIZATION California Institute of Technology 6b. OFFICE SYMBOL (If applicable)	7a. NAME OF MONITORING ORGANIZATION Rome Air Development Center (DCCD)
6c. ADDRESS (City, State and ZIP Code) Pasadena CA 91125	7b. ADDRESS (City, State and ZIP Code) Griffiss AFB NY 13441-5700
8a. NAME OF FUNDING/SPONSORING ORGANIZATION HQ Space Division 8b. OFFICE SYMBOL (If applicable) CGX	9. PROCUREMENT INSTRUMENT IDENTIFICATION NUMBER F30602-81-C-0169
8c. ADDRESS (City, State and ZIP Code) Los Angeles AFS CA 90009	10. SOURCE OF FUNDING NOS. PROGRAM ELEMENT NO. 63431F; PROJECT NO. 2028; TASK NO. 01; WORK UNIT NO. P1
11. TITLE (Include Security Classification) ADAPTIVE OPTICAL FILTERING TECHNIQUES	
12. PERSONAL AUTHOR(S) Demetri Psaltis	
13a. TYPE OF REPORT Final 13b. TIME COVERED FROM Apr 84 TO Sep 84	14. DATE OF REPORT (Yr., Mo., Day) May 1985 15. PAGE COUNT 40
16. SUPPLEMENTARY NOTATION N/A	

17. COSATI CODES			18. SUBJECT TERMS (Continue on reverse if necessary and identify by block number)
FIELD	GROUP	SUB. GR.	
17	02	03	Optical Processing; Signal Processing; Adaptive Processing;
20	06		

19. ABSTRACT (Continue on reverse if necessary and identify by block number)

The purpose of this study was to examine the potential of using optical information processing technology for adaptive antenna beamforming and null steering. The adaptive beamforming/null steering problem consists of estimation of the covariance matrix of the noise field and inversion of the covariance matrix to obtain the antenna element weights which optimize the antenna's directional characteristics (gain pattern). This report examines the adaptive beamforming/nulling problem in view of the capabilities of optics and identifies areas where optics can be used to benefit.

Benefits and drawbacks of various optical implementations of open and closed loop adaptive algorithms are discussed as well as the issues involved with optically processing digital binary numbers. Keywords:

20. DISTRIBUTION/AVAILABILITY OF ABSTRACT UNCLASSIFIED/UNLIMITED ☐ SAME AS RPT. ☑ DTIC USERS ☐	21. ABSTRACT SECURITY CLASSIFICATION UNCLASSIFIED
22a. NAME OF RESPONSIBLE INDIVIDUAL RICHARD D. HINMAN	22b. TELEPHONE NUMBER (Include Area Code) (315) 330-3224 22c. OFFICE SYMBOL RADC (DCCD)

DD FORM 1473, 83 APR EDITION OF 1 JAN 73 IS OBSOLETE.

UNCLASSIFIED
SECURITY CLASSIFICATION OF THIS PAGE

ADAPTIVE OPTICAL FILTERING TECHNIQUES

The purpose of this study is to examine the potential of using optical information processing technology for adaptive beamforming. The adaptive beamforming problem consists of estimation of the covariance matrix of the noise field and inversion of the covariance matrix to obtain the weights for the elements of the antenna. There are numerous algorithms that have been developed for this problem. Our concern here is to examine the adaptive beamforming problem in view of the capabilities of optics and identify areas where optics can be used to benefit.

There are two basic approaches to the problem: iterative solutions and direct covariance matrix inversion. In the iterative approach, the covariance matrix is never formed and thus a direct matrix inversion operation is not required. An optimum set of weights is estimated iteratively, by adjusting each weight to minimize the degree of correlation between the output of the antenna and the signals received at the individual elements. The implementation of the algorithm requires an array of complex multipliers to set the weights and an array of multipliers/accumulators to perform the required correlation operation. Simple analog optical systems can be configured to implement the iterative algorithm. For instance an array of multipliers can be implemented by an array of LEDs imaged through a multichannel acoustooptic device. Accumulation of analog products can be optically realized by temporally integrating such

products on a temporally integrating detector array or an optically addressed spatial light modulator. The more important issue is what are the possible advantages of the optical implementation over an electronic analog solution (the approach that is primarily used now). The accuracy (which is directly related to null depth) is in general comparable since both systems are analog and have similar limitations. An advantage of the optical system is smaller size, weight and possibly cost. These factors may be quite significant in a space-borne application, but it does not appear to be significant enough to have an impact for airborne or ground based applications. The difficulty with using an analog optical system to perform adaptive beamforming for a narrowband linear antenna array is that the optical system is asked to do too little; only a relatively small one dimensional array of multipliers is needed. Normally, we apply optical signal processing techniques effectively to problems that require a much heavier processing load, thereby utilizing the full capability of optics and thus obtain a clear advantage over alternate approaches.

There are two possible extensions of the simple one dimensional adaptive array that we have considered thus far, to which optical techniques may be more effectively applied. The first is large two dimensional arrays consisting of several thousand elements and thus requiring an equal number of analog multipliers for adaptive beamforming. In this case the ease with which such large parallel arrays of analog multipliers can be

optically implemented provides a clear advantage. A second area is adaptive beamforming of relatively smaller arrays, but for broadband (spread spectrum) applications. In this case, effective interference cancellation can be achieved only by having multiple taps at each antenna element. For large signal bandwidths (several hundred MHz) in a dense interference environment we may require that each antenna element have hundreds of taps. This again leads to a requirement for very large arrays of analog multipliers. Adaptive beamforming of broadband antenna arrays is probably the most promising application of analog optical methods in this general area. We have studied this application in detail and have developed optical architectures specifically for this problem. A detailed description of this processor can be found in the papers attached as Appendices A and B to this report. Another approach to this problem is described in RADC report RADC-TR-83-156[1].

The most obvious limitation of the analog implementation (be it optical or electronic) is limited accuracy. Moreover, the low accuracy restricts the algorithmic flexibility to variations of the iterative algorithm, which has the added problem that the convergence time is a function of the eigenvalues of the noise covariance matrix. Shown in Figure 1 is a diagram reproduced from RADC report RADC-TR-81-130[2] which plots the null depth as a function of the number of bits of accuracy for several direct algorithms as well as the iterative algorithm. It is seen that for the iterative algorithm an increase in the number of bits

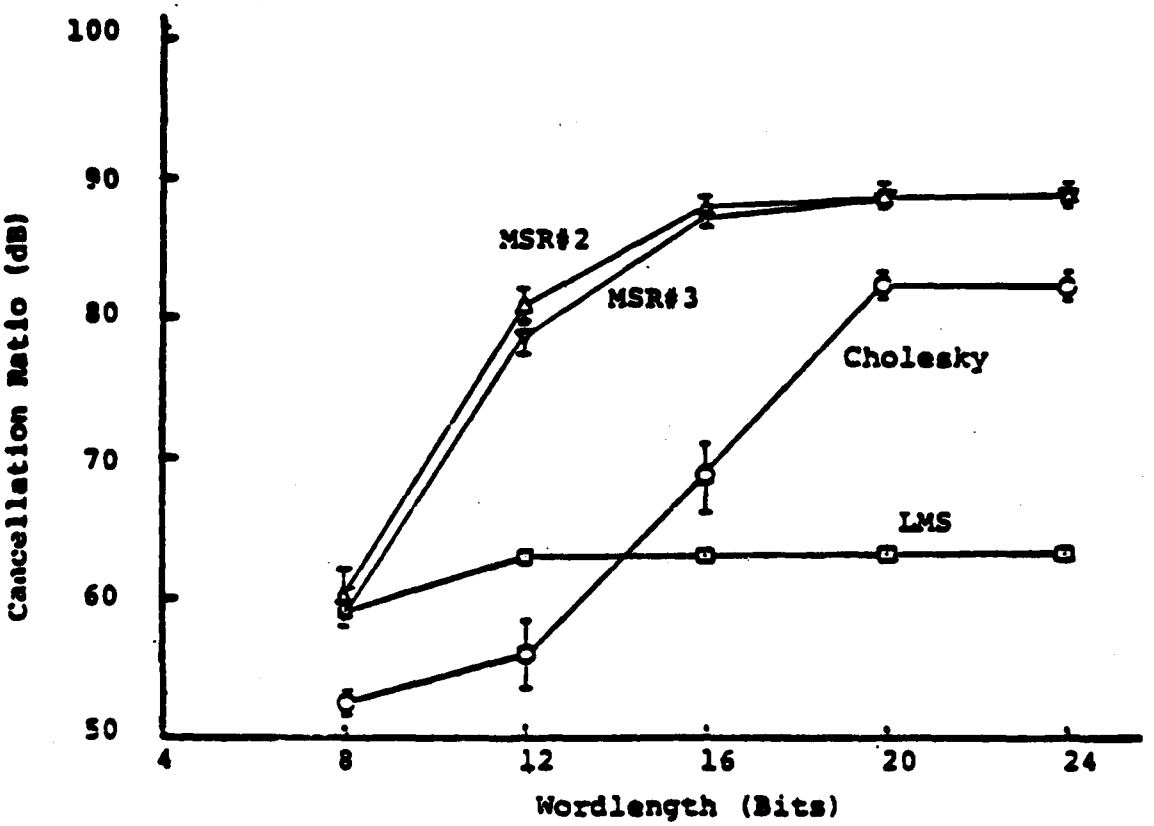

FIGURE 4-2 Cancellation Ratio Versus Wordlength for Null Steering Mode

Figure 1. Reproduced from RADC report RADC-TR-81-130 (fig.4-2)

beyond eight does not provide significant improvement in performance because the residual error due to the finite number of iterations becomes dominant. Much more effective interference suppression can be obtained with a direct algorithm if sufficient accuracy is used. The significance of this result when we consider methods for improving the performance of an optical adaptive array processor, beyond what is obtainable with an analog system, is that we must find ways to drastically improve the accuracy and also find ways to implement direct algorithms. It does not appear that we can use effectively an inaccurate optical processor that implements a direct algorithm or a very accurate one that implements an iterative algorithm. A large number of optical architectures have been developed over the last several years for performing matrix operations (vector/matrix or matrix/matrix products). These processors can in principle be applied to the implementation of direct algorithms by structuring the algorithm so that it can be implemented by successive matrix-matrix products. Direct algorithms are generally N^3 algorithms, i.e. the number of arithmetic operations required is proportional to the cube of the number of elements in the array. When we implement such an algorithm with successive matrix/matrix products, normally N such products are needed and since each matrix operation is an N^3 operation, the optical implementation requires N^4 operations to solve the N^3 problem. We have examined the possibility of optically implementing a matrix inversion with N^3 operations but we were unable to identify a viable solution. If such an implementation can be identified, then this would be a

gnificant advance since it would become much easier to obtain a eed advantage with optics. We have also examined the problem pipelining successive matrix operations as is required for the plementation of a direct matrix algorithm. A space integrating trix-matrix multiplier was developed that has the capability of lly efficient pipelining: the format of the product matrix is actly the same as that of one of the input matrices. This stem is described in the paper attached as Appendix C to the port.

The accuracy of essentially all analog matrix processors an be improved by processing digitized (binary) data through the e of the digital multiplication by analog convolution algorithm MAC). This algorithm, can provide accuracy superior to that of e analog implementation, but it reduces the processing power he maximum number of multiplications/additions that can be plemented) and increases the complexity of the post detection lectronics, since analog to digital converters are required to duce the signal produced by the optical system to true binary rmat. In what follows we examine these trade-offs.

A schematic diagram of a generalized optical processor that rforms linear operations using the DMAC algorithm is shown in g.2. The system has N_1 input parallel spatial channels and each e of these channels accepts binary bits at a rate B_1. Each annel may accept bits from a separate external information urce or alternatively, each channel accepts the bit that was at e adjacent channel during the previous cycle (one cycle=$1/B_1$

seconds). The information in each channel is multiplied by M ifferent bits in the optical processor. We call M the fan-out actor. The system has N_2 parallel output channels each having emporal bandwidth B_2. The signal detected at each output channel s then electronically converted to the binary representation by n A/D converter. Having defined these parameters we can haracterize the performance of any specific architecture without arther knowledge of the details of the implementation. Thus we ill be able to derive some guidelines that are generally pplicable. The number of "bit-multiplications" that the rocessor performs per unit time is equal to N_1B_1M. The number of it multiplications that are required to realize one ultiplication between two integers with DMAC is aK^2, where "a" s a constant between 1 and 4, depending on the efficiency of the pecific implementation, and K is the number of bits that are sed to represent each number. The processing power, P, of the verall system is:

$$P = N_1B_1M/aK^2 \text{ multiplications per second.} \quad (1)$$

learly, P is a number we wish to maximize. The number of analog o digital conversions that need to be performed per unit time s:

$$C = N_2B_2 \text{ A/D conversions per second.} \quad (2)$$

gain it is clear that C is a number we wish to minimize in order o keep the complexity of the electronicsat a minimum.

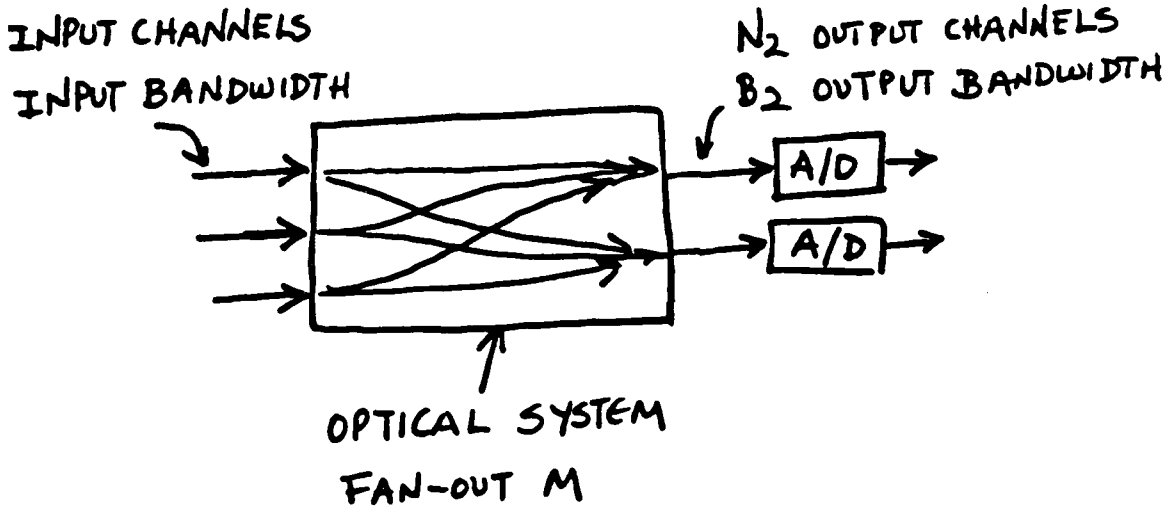

jure 2. Generalized Optical Matrix Processor Utilizing the DMAC Algorithm.

ortunately, P and C cannot be independently chosen. To reciate this fact, we define the ratio

$$R = P / C \quad \text{multiplications per A/D conversion.} \qquad (3)$$

ncreases monotonically as either P increases or C decreases, refore we want to make R as large as possible. R provides us h a direct comparative estimate of the optical implementation sus an all digital implementation. If for instance R were al to one, then only one binary multiplication is being formed by the optical system per A/D conversion. Since it is ut equally difficult to perform multiplications and A/D versions electronically, this would be a strong indication t optics offers no advantage in this case. In order to ermine the maximum value for R we consider the characteristics the output stage of the processor. The number of bits that are ng generated per unit time within the optical processor is al to aK^2P. The number of samples that are being transferred of the optical processor per unit time is C. The ratio (K^2P/C) is equal to the maximum number of bits that is umulated (through either spatial or temporal integration) to m each output sample. Therefore, this ratio cannot exceed the put dynamic range of the system, DR_2, which is defined as the ber of distinguishable signal levels that are produced by the tector and A/D converter. This gives us a very simple upper nd for R:

$$R < DR_2/aK^2. \qquad (4)$$

of the array and also is the temporal reference signal used for the detection of ed signal, s(t). It can be derived by feeding a tapped delay line with s(t); the om the ith tap corresponds to $s_i(t)$ and the tap spacing is adjusted to obtain the ok direction:

$$= s(t-i\Delta) = s(t-i(d/c)\cos\alpha), \tag{9}$$

s the desired look angle from boresight, d is the array element spacing, and c is of light.

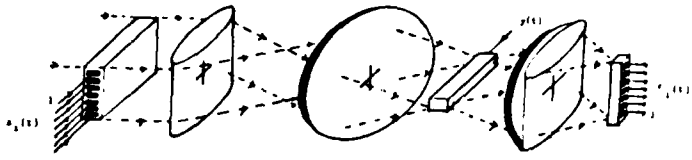

Fig.9 Multi-Channel Acoustooptic Correlator

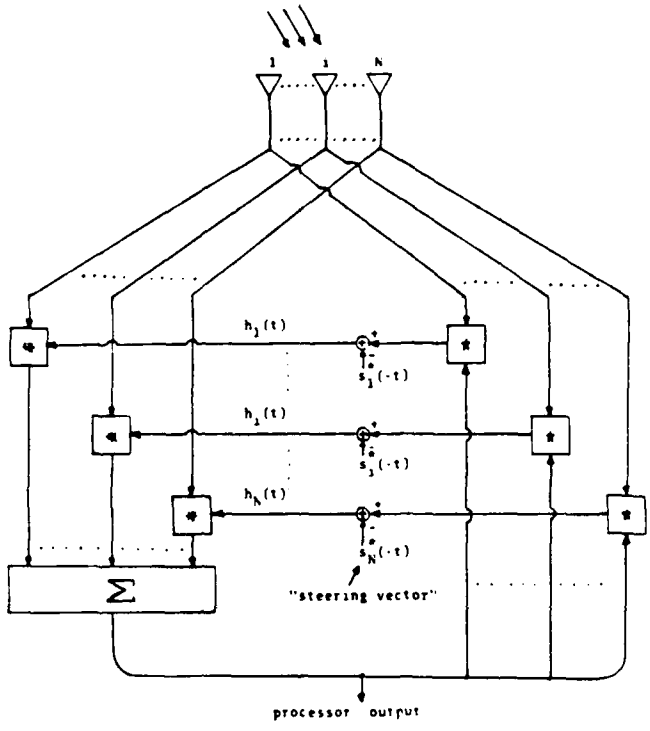

Fig.10 Broadband Adaptive Array Processor

shows the optically implemented adaptive array processor with the AOD-implemented me filter in the upper branch and the n-channel correlator in the lower one. By Eqs.(7) and (8), the equation that determines the filter function, $h_i(t)$ is seen

$$s_i^*(-t)-(G/T^2)\sum_{i=1}^{N}\int\!\!\int_{-T/2}^{T/2} x_i^*(t+2\beta)x_j(t-\tau+\beta)h_j(t+\tau+\beta)d\beta d\tau, \tag{10}$$

is the feedback gain. Under conditions of low input SNR and large feedback gain[4], an be transformed to the frequency domain to yield

$$\sum_{j=1}^{N} H_j(\omega)\int_{-\infty}^{\infty} N_i^*(\omega_1)N_j(\omega_1)\mathrm{sinc}^2[(\omega-\omega_1)T/(2\pi)]d\omega_1 \cong S_i^*(\omega), \tag{11}$$

ical processors are particularly attractive candidates for adaptive broadband array l processing because of their inherent, multidimensional processing capability. ver, the broadband requirement can be met by the use of broadband multi-channel AOD's; arge time-bandwidth products that are available translate to the possibility of nenting very high order transversal filters. The acoustooptic processor which we now ibe is an extension of the active temporal processor described earlier, to the space- domain. Here, we employ a combination of multi and single channel AOD's to perform equired operations.

e output of a general, space-time filter, with a finite accumulation time can be ssed as

$$t) = \sum_{i=1}^{N} \int_{-T/2}^{T/2} x_i(\tau) h_i(t-\tau)\, d\tau, \tag{4}$$

$x_i(t)$ is the signal from the ith antenna element, and $h_i(t)$ is the filtering function ch channel. A similar expression is obtained for the optically implemented space-time r using two multi-channel AOD's shown in Fig.8. The output of this filter is

$$t) = \sum_{i=1}^{N} (1/T) \int_{-T/2}^{T/2} x_i(t-\tau) h_i(t+\tau)\, d\tau, \tag{5}$$

we see that the only difference from the general filter (Eq.4) is in the time ession of the output. It can be shown that the optimum choice for $h_i(t)$ in Eq.(5) fies the system of integral equations:

$$\int_{-T/2}^{T/2} h_j^*(t+\tau') \gamma_{ij}(\tau-\tau')\, d\tau' = \lambda s_i(t-\tau), \tag{6}$$

$s_i(t)$ is the desired signal vector and $\gamma_{ij}(t)$ is the covariance matrix of the input given by

$$_{ij}(\tau) = E\,[n_i(t) n_j^*(t-\tau)]. \tag{7}$$

is the noise vector appearing at the array elements.

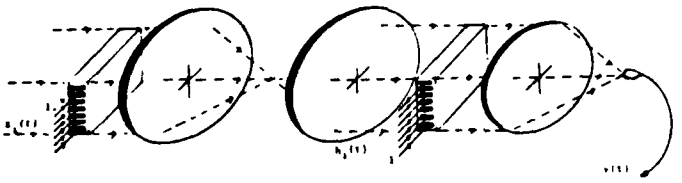

Fig.8 Acoustooptic Space-Time Filter

or adaptivity, we need to calculate and continuously update the filter function $h_i(t)$ rive the output to the optimum result. As with the previously described Active essor, the output must be correlated with the input to produce the appropriate filter tion. Since the array processor has n inputs and one output, this requires that we elate n signals with a common one. This can be achieved with the arrangement shown in which shows the use of a multi-channel AOD driven by the n antenna element outputs, onjunction with a single channel AOD which is driven by the array output signal. ifically, the output of the ith element of the linear detector array of the correlator ven by

$$_i(t) = (1/T) \int_{-T/2}^{T/2} y(t+\tau) x_i^*(t+2\tau) d\tau. \tag{8}$$

proper correlation to appear at each output, the signal driving the single channel AOD be time-compressed by a factor of two. This is indeed the case for the system ribed, and thus, the AOD implemented space-time filter and the n-channel correlator a single reference are compatible.

hown in Fig.10 is the array processor system diagram that shows the interconnections are required; it is a direct extension of the Active Processor to 2-dimensions. The ut from each antenna element is correlated with the processor output to produce the er function for that element. The steering vector, $s_i(-t)$, determines the look

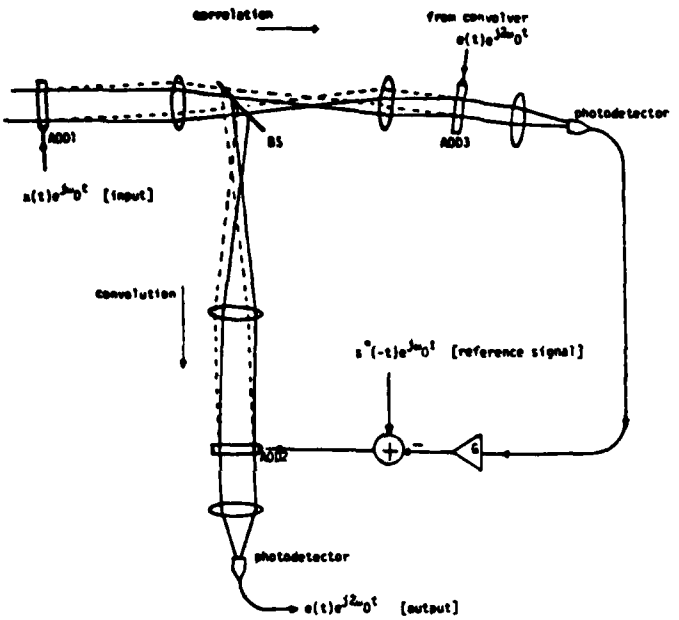

Fig.6 Adaptive Optical Processor (Active)

III. Adaptive Acoustooptic Array Processor

general adaptive scheme is shown in Fig.7 in which each channel corresponding to one element is filtered by a transversal filter with n controllable tap weights; if the has N antenna elements, then the array processor requires the adaptive control of nN endent weights. Therefore, the computational load for broadband adaptive phased array essing is much heavier than that for adaptive temporal filtering because here, the processor must adapt in two independent dimensions: space and time.

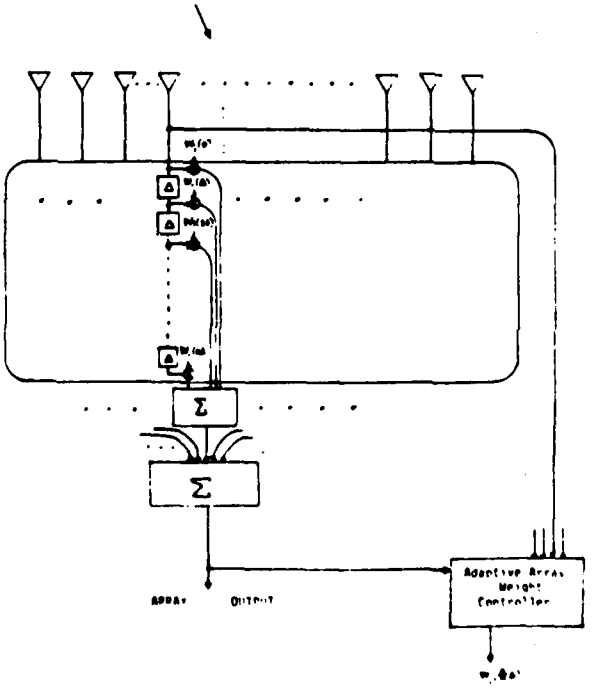

Fig.7 General Adaptive Array Processing Scheme

Correlation can be performed with the convolution configuration just described by time-eversing the input to one of the AOD's. This, however, is not acceptable for real-time peration. Shown in Fig.4 is a space-integrating processor which provides the relative iotion between the two input signals that is required for correlation by using a lemagnifying system between the two AOD's. The diffracted light from the first AOD is maged with a 2:1 magnification onto the second AOD, and the diffracted light from both .OD's is spatially integrated onto a single detector. If the input to the second AOD is ime-compressed by a factor of two, i.e., $i_4(t) = i_5(2t)$, then the correlator yields

$$I_2(t) = \int_{-T/4}^{T/4} i_3^*(t+2\tau) i_4(t+\tau)\,d\tau = \int_{t-T/2}^{t+T/2} i_3^*(\tau) i_5(t+\tau)\,d\tau, \qquad (3)$$

is its output. The above is seen to be a finite window correlation of the two signals, $i_3(t)$ and $i_5(t)$. The advantage of obtaining the time compressed output from the convolver is now clear, since it can be used as the input to the correlator just described and thus obtain a consistent, cascaded convolution-correlation operation.

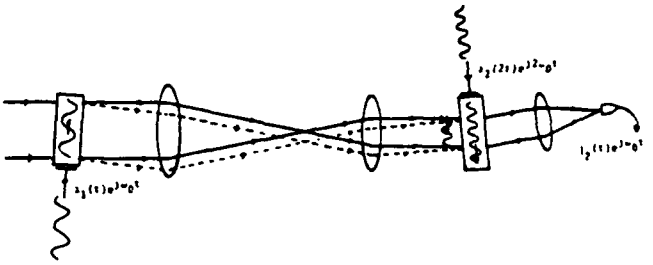

Fig.4 Space-Integrating Acoustooptic Correlator

The optical implementations of the Passive and Active Processors are shown in Figs. 5 and 6, respectively, and they differ only in their electrical interconnections. Fig. 5(6) is the system of Fig.1(2) with the optically implemented blocks of Figs. 3 and 4. In both cases, the upper branch of the processor computes the correlation while the lower performs the convolution. Since the convolver and correlator have a common input, the first AOD is shared. A more detailed description can be found in the previous publication[4].

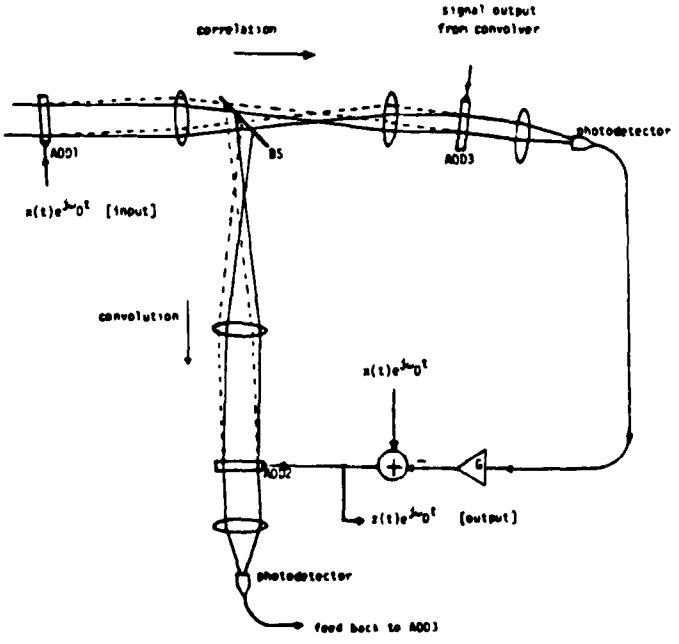

Fig.5 Adaptive Optical Processor (Passive)

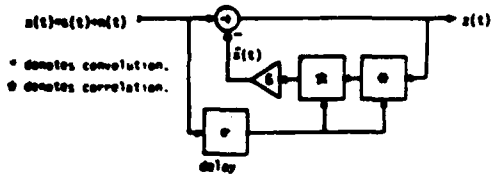

$$s(t) = z(t) - G\,[\,z(t-\sigma)*z(t)\,] * z^*(\sigma-t)$$
$$Z(\omega) = Z(\omega) / (\,1 + G|Z(\omega)|^2\,)$$
approximates the Wiener Filter for low input SNR.

Fig.1 Passive Processor

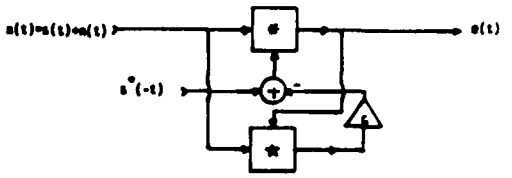

$$e(t) = z(t) * [\,s^*(-t) - Gs(t) * s^*(-t)]$$
$$E(\omega) = S^*(\omega)Z(\omega) / (\,1 + G|Z(\omega)|^2\,)$$
approximates the maximum SNR Filter for low input SNR.

Fig.2 Active Processor

For signal detection, where a known broadband signal is to be detected amidst an additive collection of narrowband jammers of unknown frequencies, a different system is required. Shown in Fig. 2 is a system diagram of such a system, the Active Processor, along with a brief, mathematical description of its operation; a complete description can be found in reference 4. As with the Passive Processor, the basic operation of this system can be understood using heuristic arguments. Suppose that the input consists soley of a large amplitude sinusoid of frequency f_0, and the desired waveform, s(t), is a broadband signal. With the loop opened at the summing junction, the output, e(t), will consist mostly of a sinusoid of frequency f_0; this signal is then correlated with the input to produce another sinusoid of the same frequency at the summing junction. When the loop is closed, the output sinusoid resulting from the convolution of the input and the code waveform, s(t), is 180° out of phase with that which is produced by the feedback signal, and hence, cancellation of the sinusoid takes place. Again, the feedback signal is negligible for small amplitude broadband signals.

Both the Passive and Active systems require convolution and correlation as the basic building blocks. In choosing the architecture to be used, we consider the following important requirements: 1)wide bandwidth, 2)dynamically controllable convolver and correlator, 3)convolver - correlator compatibility, 4)large dynamic range. These considerations lead us to choose a space-integrating acoustooptic architecture.

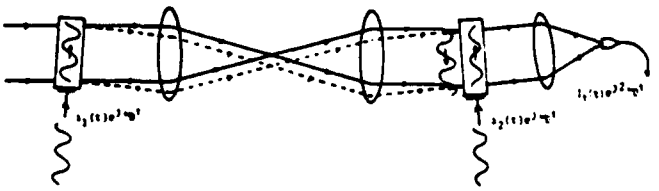

Fig.3 Space-Integrating Acoustooptic Convolver

Convolution can be performed with two AOD's as shown in Fig.3. The diffracted signal from the first AOD is imaged with unity magnification onto the second and, in the coherent realization shown, the diffracted components are spatially integrated onto a single detector whose output photocurrent is

$$I_1(t) = \int_{-T/2}^{T/2} i_1(t+\tau)i_2(t-\tau)d\tau, \quad \tau=x/v, \; T=W/2. \tag{1}$$

$i_1(t)$ and $i_2(t)$ are the complex amplitudes of the AOD input signals, v is the acoustic velocity in the AOD, and W is the physical length of the AOD aperture. This integral can be manipulated to yield the more familiar form:

$$I_1(t) = \int_{t-T/2}^{t+T/2} i_1(\tau)i_2(2t-\tau)d\tau, \tag{2}$$

which is recognized to be a finite window convolution, time-compressed by a factor of two. The seemingly troublesome compression is actually an advantage in this case as will be apparent when we consider the correlator implementation.

Appendix B

519-09

Adaptive Acoustooptic Processor

Demetri Psaltis and John Hong
Department of Electrical Engineering, California Institute of Technology
Pasadena, Calif. 91125

Abstract

Space-integrating, acoustooptic processors for adaptive, temporal filtering are examined. The basic architecture is then extended to the space-time domain for application in broadband phased array processing. An acoustooptic processor capable of such 2-dimensional, adaptive processing is described.

I. Introduction

A major portion of optimum filtering theory concerns itself with the efficient separation of useful signals from additive noise. Fixed optimum filters, such as the Wiener filter, are applicable when the signal and noise statistics are stationary and known apriori; the lack of such apriori knowledge, however, motivates the implementation of adaptive filters which estimate the required signal and noise characteristics. The implementation of such filtering techniques requires a processor which must be able to compute various correlation functions of signal and noise and change its transfer function accordingly.

The situation becomes considerably more complex when one is required to adaptively filter signals in the space-time domain, as in the case of broadband array processing. The number of broadband jammers that an adaptive processor can cancel without compromising its directional discrimination can be used as its performance measure. Electronic implementations of such array processors[1] have exhibited limited performance with respect to this measure. The transversal filters responsible for temporally filtering the outputs from the array elements are of low order and hence, operation is usually limited to narrowband signals, due to hardware limitations.

The bandwidth requirements and the parallel nature of array processing make optical implementations attractive. Various optical implementations have been explored by researchers in the area[2,3]. In a recent paper[4], we described two optical adaptive filters for use in the time domain. These implementations are strictly one-dimensional, requiring only one dimensional devices, permitting an extension to the space-time domain through the use of multi-channel AOD's. In this paper, we briefly review the operation of the temporally adaptive acoustooptic filter. After this foundation has been established, an adaptive array processor utilizing multi-channel AOD's in a space integrating architecture will be described.

II. Adaptive Temporal Filters

To be adaptive, a processor that optimizes either the mean-square error or SNR criterion must compute various correlation functions of the input signal and noise and vary its filter response characteristics accordingly. Specifically, we will consider situations where the signal is broadband and the additive noise consists of strong, narrowband jammers whose frequencies are unknown; the jammer frequencies must be estimated for effective noise rejection.

Shown in Fig.1 is a system diagram of the Passive Processor which was shown to adaptively perform an approximate Wiener filtering operation[4]. The operation of the system can be explained heuristically in the following manner. Suppose that the input consists soley of a single sinusoid, and consider the feedback signal, $\hat{s}(t)$, with the loop opened at the summing junction. The input sinusoid is first convolved with a replica of itself, delayed by ϵ to produce another sinusoid of the same frequency, also delayed by ϵ, at the input of the correlator. This is then correlated with the input delayed by ϵ to produce a sinusoid with the same phase as the input sinusoid appearing at the summing junction; the delays, ϵ, cancel out due to the cascaded correlation-convolution operations. The possibility of stable cancellation is now apparent since the two signals, the input and feedback signals, which are subtracted at the junction, are identical in frequency and phase. Cancellation does not occur for a broadband input, because it correlates poorly with delayed versions of itself, resulting in a negligible feedback signal, $\hat{s}(t)$. The passive processor thus discriminates against narrowband components of the input signal, while preserving the desired, broadband components of the input, making it suitable for signal estimation.

processor to distinguish between the various jamming signals present at the input.

The optically implemented active processor is shown schematically in Fig. 8; the active system differs from the passive only in its electrical interconnections. Here the output of the system is a time compressed signal since it is taken at the output of the convolver; this presents no problems since the output signal is a correlation peak, and we are interested in detection rather than estimation. As in the passive case, the convolver output drives AOD3 of the correlator. The correlator output is then subtracted from the time reversed reference signal (the matched filter impulse response) to form the input to AOD2 of the convolver; note that even though the output is time compressed, the time scaling is compatible for all the signals within the system. To see this more precisely, we examine the input–output equation for the active system; using Eqs. (16) and (17), we obtain

$$e(t) = (1/T)\int_{-T/4}^{T/4} x(t+\tau)s^*(\tau - t)d\tau - (G/T^2)\iint_{-T/4}^{T/4} x(t+\tau)x^*(t-\tau+2v)s(t-\tau+v)dvd\tau, \tag{23}$$

where $e(t)$ is the system output. Under low SNR conditions, Eq. (23) can be approximated by

$$e(t) \approx (1/T)\int_{-T/4}^{T/4} x(t+\tau)s^*(\tau - t)d\tau - (G/T^2)\iint_{-T/4}^{T/4} n(t+\tau)n^*(t-\tau+2v)s(t-\tau+v)dvd\tau, \tag{24}$$

The output spectrum is easily calculated from Eq. (24) to be

$$E(\omega) = \frac{(\frac{1}{2}\pi)\int_{-\infty}^{\infty} X(\alpha)S^*(\omega-\alpha)\,\mathrm{sinc}[(\omega-2\alpha)T/4\pi]d\alpha}{1+(G/4\pi^2)\int_{-\infty}^{\infty}|N(\alpha)|^2\,\mathrm{sinc}^2[(\omega-2\alpha)T/4\pi]d\alpha}. \tag{25}$$

Aside from the appearance of the sinc functions which arise due to the finite apertures of the AODs and the time compression, Eq. (25) is quite similar to Eq. (9), the matched filter result.

V. Conclusion

Two adaptive systems particularly suitable for use in narrowband jamming noise environments have been presented. The passive system has been shown to be appropriate for estimation purposes while the active, for signal detection. A particularly interesting extension of this work is the implementation of time–space adaptive filters for processing broadband signals from phased array antennas. The processors described in this paper are temporal filters, but since they are implemented in only one dimension, it is possible, through use of multiple transducer AODs, to implement a 2-D time–space adaptive filter. The 1-D processors are currently being built in the laboratory, and future research will include the experimental verification of the operation of the systems as well as statistical characterization of the effects of the finite apertures of the AODs and detector noise.

This work is supported by the Rome Air Development Center.

References

1. A. P. Appelbaum, "Adaptive Arrays," IEEE Trans. Antennas. Propag. AP-24, 585 (1976).
2. B. Widrow, P. E. Mantey, L. J. Griffiths, and B. B. Goode, "Adaptive Antenna Systems," Proc. IEEE 55, 2143 (1976).
3. K. K. Scott, "Transversal Filter Techniques for Adaptive Array Applications," Proc. IEE 130, Parts F+H, 29 (Feb. 1983).
4. R. Riegler and R. Compton, Jr., "An Adaptive Array for Interference Rejection," Proc. IEEE 61, 748 (1973).
5. R. W. Lucky, "Adaptive Redundancy Removal in Data Transmission," Bell Syst. Tech. J. 47, 549 (1968).
6. M. M. Sondhi, "An Adaptive Echo Canceller," Bell Syst. Tech. J. 46, 497 (1967).
7. B. Widrow *et al.*, "Adaptive Noise Cancelling: Principles and Applications," Proc. IEEE 63, 1692 (1975).
8. D. R. Morgan and S. E. Craig, "Real Time Adaptive Linear Prediction Using the Least Mean Square Gradient Algorithm," IEEE Trans. Acoust. Speech, Signal Process. ASSP-24, 494 (1976).
9. J. E. Bowers, G. S. Kino, D. Behar, and H. Olainen, "Adaptive Deconvolution Using SAW Storage Correlators," IEEE Trans. Microwave Theory Tech. MTT-29, 491 (1981).
10. L. J. Griffiths, "Rapid Measurement of Instantaneous Frequency," IEEE Trans. Acoust. Speech, Signal Process. ASSP-23, 209 (1975).
11. J. Koford and G. Grover, "The Use of An Adaptive Threshold Element to Design a Linear Optimal Pattern Classifier," IEEE Trans. Inf. Theory IT-12, 42 (1966).
12. A. Papoulis, *Probability, Random Variables, Stochastic Processes* (McGraw-Hill, New York, 1965).
13. M. White, I. A. Mack, G. M. Borsuk, D. R. Lampe, and F. J. Kub, "CCD Adaptive Discrete Analog Signal Processing," IEEE J. Solid-State Circuits SC-14, 132 (1979).
14. C. F. N. Cowan, J. W. Arthur, J. Mavor, and P. B. Denyer, "CCD Based Adaptive Filters: Realization and Analysis," IEEE Trans. Acoust. Speech Signal Process ASSP-29, 220 (1981).
15. D. Psaltis *et al.*, "Iterative Color-Multiplexed Electrooptical Processor," Opt. Lett. 4, 348 (1979).
16. D. Psaltis *et al.*, "Iterative Optical Processor for Adaptive Phase Array Radar Applications," Proc. Soc. Photo-Opt. Instrum. Eng. 180, 114 (1979).
17. J. F. Rhodes, "Adaptive Filter with a Time-Domain Implementation Using Correlation Cancellation Loops," Appl. Opt. 22, 282 (1983).
18. A. VanderLugt, "Adaptive Optical Processor," Appl. Opt. 21, 4005 (1982).
19. J. N. Lee, N. J. Berg, and P. S. Brody, "High Speed Adaptive Filtering and Reconstruction of Broadband Signals Using Acoustooptic Techniques," in *Proceeding, Ultrasonics Symposium* (1980), pp. 488–491.
20. W. Davenport and W. Root, *Introduction to Theory of Random Signals and Noise* (McGraw-Hill, New York, 1987).
21. A. Yariv, *Quantum Electronics* (Wiley, New York, 1967).
22. W. T. Rhodes, "Acousto-Optic Signal Processing: Convolution and Correlation," Proc. IEEE 69, 65 (1981).

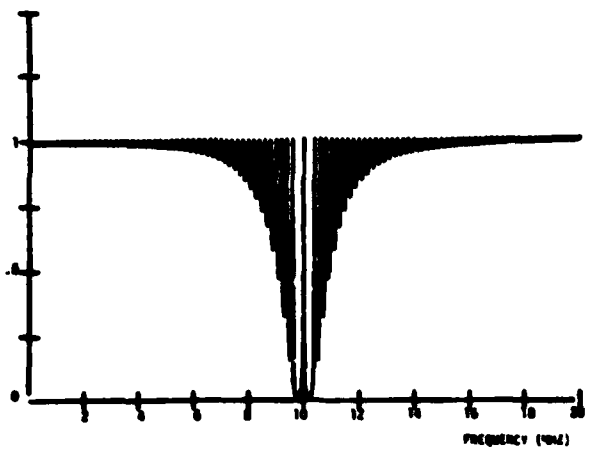

Fig. 6. Passive processor response to two jammers: $f_1 = 9.8$ MHz, $f_2 = 10.2$ MHz, $T = 10$ μsec.

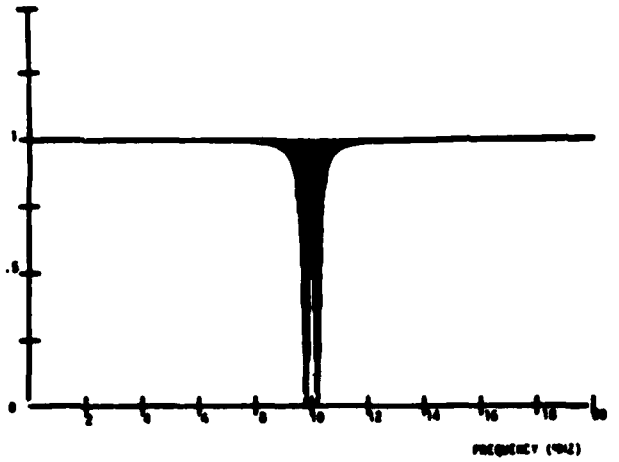

Fig. 7. Passive processor response to two jammers: $f_1 = 9.8$ MHz, $f_2 = 10.2$ MHz, $T = 50$ μsec.

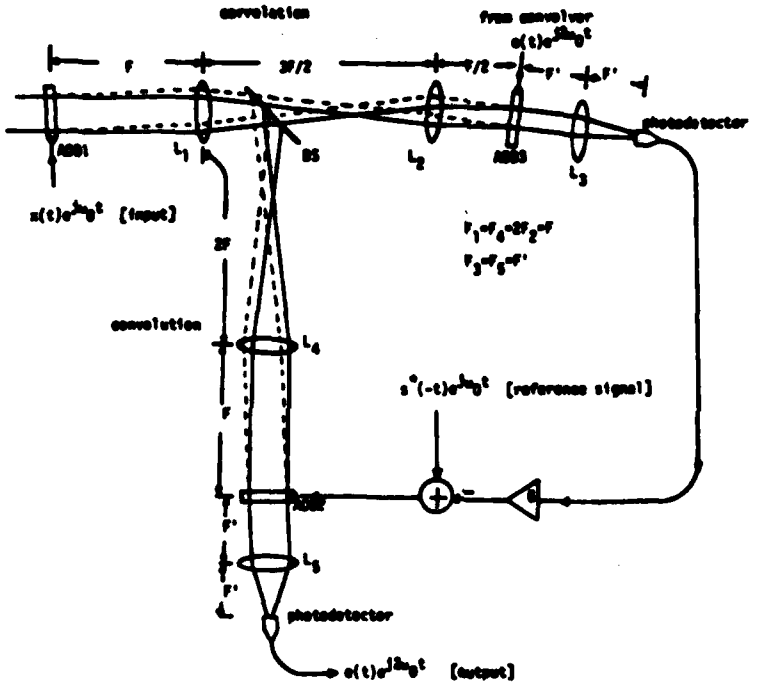

Fig. 8. Adaptive optical processor (active).

$$Z(\omega) = X(\omega) - (G/4\pi^2)\iint_{-\infty}^{\infty} N^*(\alpha) \times N(\beta)\exp[-j(\beta-\alpha)\sigma]Z(\omega+\alpha-\beta) \times \operatorname{sinc}[(\omega-\alpha)T/4\pi]\operatorname{sinc}[(\omega+\alpha-2\beta)T/4\pi]d\alpha d\beta. \quad (20)$$

The double integral of (20) can be approximated by a single integral since it becomes appreciably large only near the region $\alpha = \beta$, so that

$$Z(\omega) = X(\omega) - (G/4\pi^2)Z(\omega)\int_{-\infty}^{\infty}|N(\alpha)|^2 \times \operatorname{sinc}^2[(\omega-\alpha)T/4\pi]d\alpha. \quad (21)$$

Solving for $Z(\omega)$ gives

$$Z(\omega) = \frac{X(\omega)}{1 + (G/4\pi^2)\int_{-\infty}^{\infty}|N(\alpha)|^2\operatorname{sinc}^2[(\omega-\alpha)T/4\pi]d\alpha}. \quad (22)$$

Except for the presence of the sinc function in the denominator due to the finite apertures of the AODs, Eq. (22) is quite similar to the Wiener result, Eq. (6). Shown on Figs. 6 and 7 are plots of $Z(\omega)/X(\omega)$ for an input consisting of two sinusoids, one at 9.8 MHz and the other at 10.2 MHz; the first plot is for $T = 10$ μsec, while the second is for $T = 50$ μsec. Clearly, the finite aperture of the AODs limit the resolving power of the

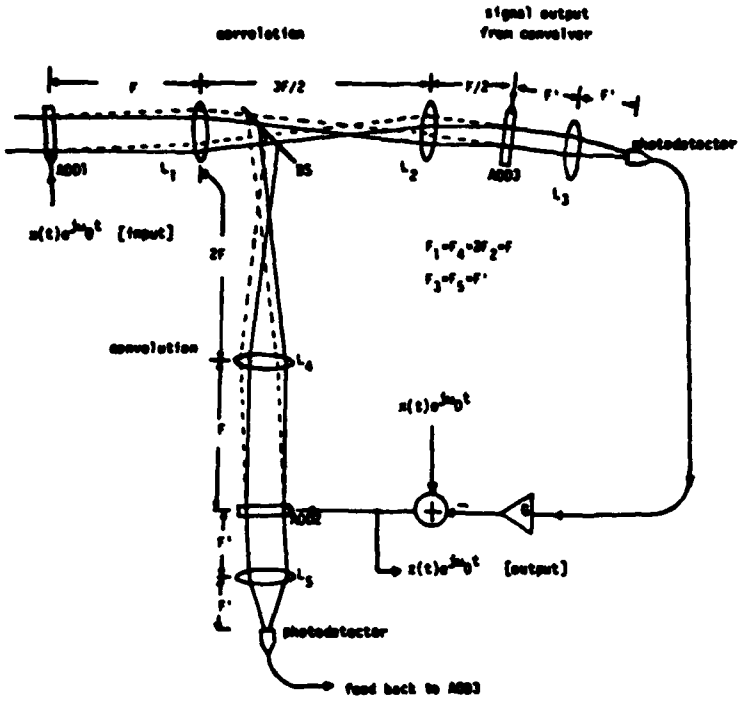

Fig. 5. Adaptive optical processor (passive).

been incorporated into one system requiring only one light source and three AODs. The correlator and convolver share, in effect, the AOD which is driven by the system input signal $x(t)$. The input signal, translated in frequency to ω_0, is applied to AOD1 and the summing node before entering AOD2. The convolution is performed by the lower leg of the processor and the correlation by the upper leg. As shown in the previous section, the optical convolver takes its two inputs, each at the carrier frequency ω_0 and gives their convolution, compressed in time by a factor of 2 and translated to $2\omega_0$, as its output. This output is then used to drive AOD3 of the correlator; recalling that to achieve a proper correlation, one of the correlator inputs must be time compressed by a factor of 2 and translated to $2\omega_0$, we see that its output is free of time scaling problems. This signal is then subtracted from the input signal to form the system output $z(t)$ which is fed back to the convolver via AOD2. The delay element which is necessary in the passive processor can be realized simply by translation of AOD1 along the direction in which the acoustic signal propagates.

We now derive the output of the optical passive processor that is obtained under the conditions stated in Sec. II. We begin by stating the mathematical operations performed by the optically implemented blocks of Figs. 1 and 2; with i_1 and i_2 as the inputs of the blocks, the convolver block output is given by

$$u(t) = (1/T)\int_{-T/4}^{T/4} i_1(t+\tau)i_2(t-\tau)d\tau, \tag{16}$$

and the correlator block output is given by

$$w(t) = (1/T)\int_{-T/4}^{T/4} i_1^*(t+2\tau)i_2(t+\tau)d\tau. \tag{17}$$

Equations (16) and (17) are simply Eqs. (13) and (14), respectively, with the carrier frequencies suppressed. These integals are different from their counterparts found in Eqs. (1) and (2) in two important ways. First, Eqs. (16) and (17) have finite limits of integration limited by the maximum transit delay time of the AODs. Also the arguments of the integrand are different, and these differences reflect the time compression problems of the optical convolver and correlator referred to earlier. In both cases, the integration limits extend from $-T/4$ to $T/4$, where T is the aperture of each AOD in units of time. With Eqs. (16) and (17), the input–output equation of the passive processor is

$$z(t) = x(t) - (G/T^2)\iint_{-T/4}^{T/4} x^*(t+2v-\sigma) \times x(t+\tau+v-\sigma)x(t-\tau+v)d\tau dv, \tag{18}$$

where, as in Sec. II, $z(t)$ is the system output, and $x(t) = s(t) + n(t)$ is the input; $s(t)$ is the broadband signal, and $n(t)$ is the narrowband interference. The delay element σ causes the broadband components to become decorrelated so that the narrowband components dominate the double integral of Eq. (18) yielding

$$z(t) = x(t) - (G/T^2)\iint_{-T/4}^{T/4} n^*(t+2v-\sigma) \times n(t+\tau+v-\sigma)x(t-\tau+v)d\tau dv. \tag{19}$$

Fourier transformation then yields

of the AOD; note that the Bragg condition, Eq. (10), was used to derive the last line of Eq. (11). The first term on the right-hand side of Eq. (11) corresponds to the dc or undiffracted light which is unmodulated to first order. The second term corresponds to the (−1) diffracted order, which is modulated by $a_1^*(t - x/v)$, Doppler shifted by $-\omega_0$, and deflected by an angle $2\theta_B$. The amplitude distribution, $A_1(x,t)$ in Eq. (11), is then imaged onto the second AOD by lenses $L1$ and $L2$; the imaging reverses the spatial coordinate x. The second AOD is positioned at the Bragg angle with respect to the dc component from AOD1, and, therefore, a portion of it is diffracted at an angle $2\theta_B$ by AOD2. The major portion of the diffracted beam from AOD1 passes through AOD2 undiffracted, since it is not Bragg-matched, and it propagates in the same direction as the beam diffracted by AOD2. The remaining components of the light at the exit of AOD2 are angularly separated from these two components and, therefore, can be blocked at the focal plane of lens $L3$. The two components of interest are given by

$$A_2(x,t) \propto [a_2(t - x/v)\exp(-j2\pi \sin\theta_B x/\lambda)\exp(j\omega_0 t) + a_1^*(t + x/v)\exp(-j2\pi \sin\theta_B x/\lambda) \times \exp(-j\omega_0 t)]\,\mathrm{rect}(x/W). \quad (12)$$

The first term on the right-hand side of Eq. (12) is the (+1) diffracted order from AOD2, which is modulated by $a_2(t - x/v)$, Doppler shifted by ω_0, and deflected from the dc by $2\theta_B$; this beam is collinear with the (−1) diffracted beam from AOD1 [i.e., the second term in Eq. (12)]. The light amplitude at the back focal plane of lens $L3$ is the Fourier transform of Eq. (12). A detector with an active area sufficiently large to integrate the entire transform is placed at the Fourier plane, and the resulting photocurrent is

$$I_1(t) \propto \int_{-T/2}^{T/2} |a_1(t + \tau)|^2 d\tau + \int_{-T/2}^{T/2} |a_2(t - \tau)|^2 d\tau + 2\,\mathrm{Re}\left\{\exp(j2\omega_0 t)\int_{-T/2}^{T/2} a_1(t + \tau)a_2(t - \tau)d\tau\right\}. \quad (13)$$

where $\tau = x/v$, and T is the acoustic delay through the aperture of the AOD, i.e., $T = W/v$. The first two terms on the right-hand side of Eq. (13) are low frequency components, and they are removed by filtering. The third term is the desired operation which is the convolution of $a_1(t)$ and $a_2(t)$. The convolution is compressed in time by a factor of 2 and translated to twice the original carrier freqeuncy. Notice that in both passive and active processors, the time compressed output of the convolver is one of the inputs to the correlator. Thus the correlator must be designed to accept a time compressed signal (by a factor of 2) in one of its input ports.

In contrast to convolution which requires an inversion of a coordinate, correlation requires that one of the input signals be in motion with respect to the other with no coordinate inversion. Referring to Fig. 4, the correlator consists of two identical AODs with counter-propagating acoustic signals; ω_0 and $2\omega_0$ are the carrier frequencies of the signals driving AOD3 and AOD4, respectively. The imaging system reverses the spatial

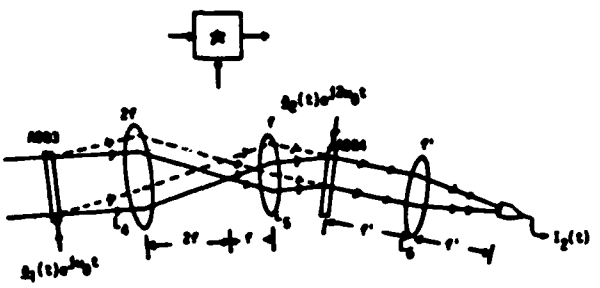

Fig. 4. Space integrating optical correlator.

coordinate of the signal in AOD3, so that the two signals are copropagating at AOD4. The imaging system has a 2:1 demagnification ratio, so that the velocity of the image of the light that is diffracted by AOD3 is half of that of the acoustic signal in AOD4. Thus the signals in the AODs continuously translate with respect to each other. The undiffracted beam from AOD3 is incident at the Bragg angle of AOD4 corresponding to its $2\omega_0$ center frequency. The demagnification by a factor of 2 increases the angular separation between the diffracted and undiffracted beams from AOD3 at the plane of AOD4. Therefore, the two diffracted beams from AOD3 and AOD4 are parallel to one another when they enter lens $L6$. $L6$ forms the Fourier transform of the light exiting AOD4, and a photodetector spatially integrates the entire spectrum. Through a development similar to that illustrated for the convolver, we find that the photocurrent from the detector in Fig. 4 is

$$I_2(t) \propto \int_{-\infty}^{\infty}\left|\int_{-T/4}^{T/4}[a_1(t + 2\tau)\exp(j\omega_0 t) + a_2(t + \tau)\exp(j2\omega_0 t)]\exp(jk\tau)d\tau\right|^2 dk \propto \int_{-T/4}^{T/4}|a_1(t + 2\tau)|^2 d\tau + \int_{-T/4}^{T/4}|a_2(t + \tau)|^2 d\tau + 2\,\mathrm{Re}\left\{\exp(j\omega_0 t)\int_{-T/4}^{T/4} a_1^*(t + 2\tau)a_2(t + \tau)d\tau\right\}, \quad (14)$$

where k is the spatial frequency variable at the output plane. The limits of integration of the correlator are half of those of the convolver. This implies that the apertures of the AODs used in the correlator must be twice as long as those in the convolver to obtain equal integration limits. Unilluminated portions of the AODs in the correlator and the convolver can be used for introducing delays. The third term is the desired operation which resembles a correlation translated to the carrier frequency ω_0. If $a_2(t) = a_3(2t)$, the third term of Eq. (14) becomes

$$= 2\,\mathrm{Re}\left\{\exp(j\omega_0 t)\int_{t-T/2}^{t+T/2} a_1^*(\alpha)a_3(t + \alpha)d\alpha\right\}, \quad (15)$$

which is a finite aperture correlation of the signals $a_1(t)$ and $a_3(t)$ placed on the carrier frequency ω_0.

IV. Adaptive Optical Processor Implementations

A schematic diagram of the optically implemented passive processor is shown in Fig. 5. Through use of a beam splitter, both the convolver and correlator have

The Fourier transform of the output signal $e(t)$ is readily found to be

$$E(\omega) = \frac{X(\omega)S^*(\omega)}{1 + G|N(\omega)|^2} \approx \frac{X(\omega)S^*(\omega)}{G|N(\omega)|^2}, \tag{9}$$

where $E(\omega)$ is the Fourier transform of $e(t)$, and the last result is valid if the feedback gain G is made sufficiently large. If the input SNR is high, it is evident from the equations that the system will equalize the spectrum of the total input signal while simultaneously performing a matched filtering operation. Identifying $|N(\omega)|^2$ as the power spectrum of the noise, Eq. (9) is the matched filter result.[20] Thus, from Eqs. (6) and (9), both active and passive processors share the common property of suppressing strong narrowband components that are present in the input signal. This property, commonly called line cancellation, is suitable in environments where sinusoidal jammers are present for either estimation or detection of broadband spread spectrum signals.

III. Optical Filters

The two adaptive filters that we described in the previous section are both implemented with a convolver and a correlator. There are several possible ways to implement an optical correlator/convolver. In selecting an implementation that is best suited for this application, we must consider the following requirements: (a) The optical filters should be capable of processing broadband signals (1-GHz bandwidth) to be applicable to spread spectrum systems. This requirement suggests an acoustooptic implementation. (b) The impulse response of the convolver and the correlator must be dynamically controllable. The impulse response of the correlator, in particular, is also a broadband signal. (c) The two filters must be compatible with one another; the impulse response of the convolver is determined by the output of the correlator, and the output of the convolver is one of the inputs to the correlator. (d) We must select architectures that have the maximum linear dynamic range possible. Adaptive filters are typically used to process signals with very low SNRs; this implies that they must have a sufficient dynamic range to place very deep nulls at the frequencies where the interference occurs in order to suppress it effectively. The acoustooptic space integrating convolver, consisting of two counterpropagating AODs, an integrating lens, and a single detector, is well suited for this application in that its two inputs and the output are broadband electrical signals, and a very high dynamic range is possible in this architecture. One potential difficulty with using this type of convolver is the fact that its output is time-compressed by a factor of 2, and thus it cannot be directly correlated with the input signal as required for adaptive filtering. A second problem is that correlation cannot be readily performed with this architecture; one of the input signals must be time reversed before it is applied to the convolver to compute the correlation with such a system. These two

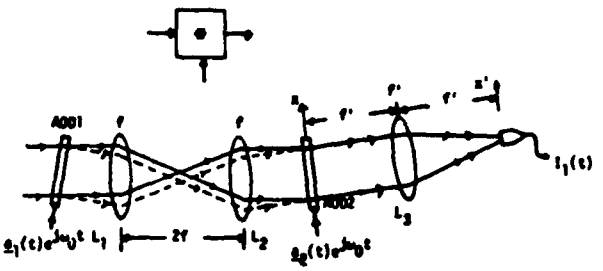

Fig. 3. Space integrating optical convolver.

problems combine to provide a solution in this case. We will show that a space integrating correlator can be implemented with two copropagating AODs if one of the inputs to the correlator is time compressed. The output of the space integrating convolver can thus be used as one of the inputs to such a correlator. In this section we describe a specific coherent realization of the acoustooptic convolver and correlator blocks. Several variations of these processors are possible, including an incoherent implementation. We begin with the description of the convolver shown in Fig. 3. It consists of two AODs with copropagating acoustic signals. The 1:1 imaging system between the AODs provides the coordinate inversion of one signal with respect to the other which is necessary for the convolution. Let $s_1(t)$ and $s_2(t)$ which are of the form, $s(t) = a(t)\cos[\omega_0 t + p(t)] = \mathrm{Re}[\mathbf{a}(t)\exp(j\omega_0 t)]$, represent the signals applied to the AODs; the complex envelope, $\mathbf{a}(t) = a(t)\exp[jp(t)]$, is the modulating signal, and ω_0 is the center frequency of the AODs. The first AOD in Fig. 3 is illuminated by a collimated coherent light beam incident at the Bragg angle θ_B (Ref. 21):

$$\sin\theta_B = \lambda\omega_0/4\pi v, \tag{10}$$

where λ is the wavelength of light in the acoustooptic crystal, and v is the speed of sound in the crystal.

The interaction between the acoustic wave induced by the signal $s_1(t)$ and the optical field causes some of the incident light to be diffracted, and since the AODs are operated in the Bragg regime, only first-order diffraction is appreciable. For a more compact analysis, the induced acoustic signal in the AOD is treated as the system input; i.e., the fixed delay between the applied electrical signal and the acoustic signal is ignored. The final results, however, are strictly equivalent. In the actual implementation, additional delays will be necessary to compensate for the delays intrinsic to the acoustooptic system. For weak modulation, the optical field at the exit plane of AOD1 is given by[22]

$$\begin{aligned} A(x,t) &\propto \{\exp(-j2\pi\sin\theta_B x/\lambda) \\ &\quad + j(m/2)\mathbf{a}[(t - x/v)\exp[-j\omega_0(t - x/v)] \\ &\quad \times \exp(-j2\pi\sin\theta_B x/\lambda)\}\,\mathrm{rect}(x/W) \\ &\propto \{\exp(-j2\pi\sin\theta_B x/\lambda) + j(m/2)\mathbf{a}[(t - x/v)\exp(-j\omega_0 t) \\ &\quad \times \exp(j2\pi\sin\theta_B x/\lambda)\}\,\mathrm{rect}(x/W), \end{aligned} \tag{11}$$

where m is a constant, x is along the direction of the acoustic wave propagation, and W is the aperture size

presence of additive noise, but it requires that the autocorrelations as well as the cross-correlation of the signal and the noise be known in advance. The filter that maximizes the output SNR is the matched filt r which requires prior knowledge of the autocorrelation of the noise and also the desired signal waveform.

When the necessary correlation functions are not known *a priori*, they must be estimated adaptively from the past history of the signal and the limited and qualitative information that is available. We assume that the available information is as follows: the signal and noise are uncorrelated, and the signal is broadband, as in spread spectrum systems. We model the wideband signal as bandlimited white noise, so that $S_s(\omega)$, the spectral density of the wideband signal $s(t)$, is equal to $S_0 \operatorname{rect}[(\omega - \omega_0)/\Delta\omega]$, where ω_0 is the center frequency of the signal and $\Delta\omega$ is its bandwidth. The spectral density of the interference $n(t)$ is assumed to be unknown, and it is adaptively estimated.

Shown in Fig. 1 is a system diagram of the passive processor, which will be shown to adaptively perform an operation that approximates the Wiener filter under the conditions stated in the above paragraph. The two necessary operations in implementation of this filter are a convolution and a correlation. The convolver serves as the variable filter that is controlled by the correlator which estimates the correlation of the interference. The operation of the convolver and correlator blocks are described by the following input–output relations:

$$u(t) = \int_{-\infty}^{\infty} i_1(t-\tau) i_2(\tau)\, d\tau, \tag{1}$$

$$w(t) = \int_{-\infty}^{\infty} i_1(t+\tau) i_2^*(\tau)\, d\tau, \tag{2}$$

where $i_1(t)$ and $i_2(t)$ are the inputs to the blocks. Using Eqs. (1) and (2), we find the relationship between the input and output signals, $x(t)$ and $z(t)$, respectively, of the passive processor of Fig. 1:

$$\begin{aligned} z(t) &= x(t) - G \iint_{-\infty}^{\infty} z(\tau) x^*(\alpha-\sigma) x(t+\alpha-\tau-\sigma)\, d\alpha\, d\sigma\, d\tau \\ &= x(t) - G \iint_{-\infty}^{\infty} z(\tau) [s^*(\alpha-\sigma) + n^*(\alpha-\sigma)] \\ &\quad \times [s(t+\alpha-\tau-\sigma) + n(t+\alpha-\tau-\sigma)]\, d\alpha\, d\sigma\, d\tau, \end{aligned} \tag{3}$$

where σ is a time delay. Low input SNR, along with the assumption of the uncorrelatedness between the signal $s(t)$ and the noise $n(t)$, results in the reduction of Eq. (3) into

$$z(t) \approx x(t) - G \iint_{-\infty}^{\infty} z(\tau) n^*(\alpha-\sigma) n(t+\alpha-\tau-\sigma)\, d\alpha\, d\sigma\, d\tau. \tag{4}$$

Fourier transformation of the above equation yields the approximate steady-state description:

$$Z(\omega) \approx X(\omega) - GZ(\omega)|N(\omega)|^2, \tag{5}$$

where $Z(\omega)$ and $X(\omega)$ are the Fourier transforms of $z(t)$ and $x(t)$, respectively, and $|N(\omega)|^2$ is the power spectrum of a sample realization of $n(t)$. Solving for $Z(\omega)$ gives

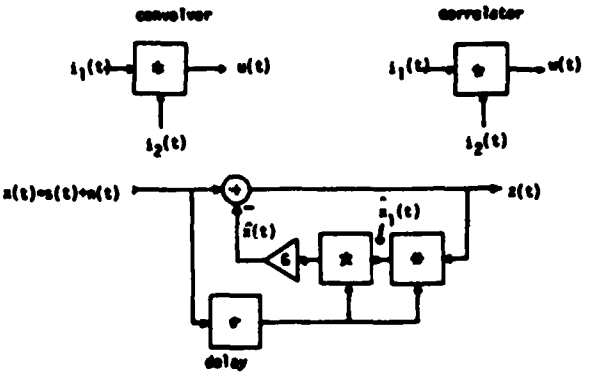

$$\hat{n}_1(t) = \int_{-\infty}^{\infty} x(t-\sigma-\tau) z(\tau)\, d\tau$$

$$\hat{x}(t) = G \int_{-\infty}^{\infty} x^*(\alpha-\sigma) n_1(t+\alpha)\, d\alpha = G \iint_{-\infty}^{\infty} x^*(\alpha-\sigma) x(t+\alpha-\sigma-\tau) z(\tau)\, d\alpha\, d\tau$$

Fig. 1. Passive processor.

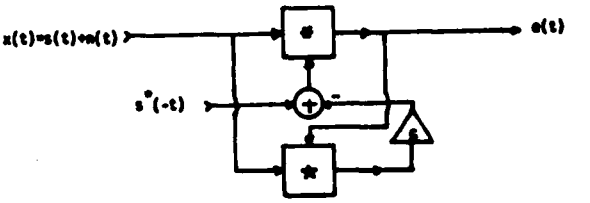

Fig. 2. Active processor.

$$Z(\omega) \approx \frac{X(\omega)}{1 + G|N(\omega)|^2} = \frac{1/G}{1/G + |N(\omega)|^2} X(\omega). \tag{6}$$

The input signal to the convolver and the correlator in Fig. 1 is delayed by the same amount, and, therefore, the output of the convolver–correlator combination $\hat{x}(t)$ becomes independent of the delay. This is an important result since it assures that the feedback signal $\hat{x}(t)$ is inphase with the input signal, and hence the system will be stable. With $G = 1/S_0$ and identifying $|N(\omega)|^2$ as the estimate of $S_n(\omega)$, the spectral density of $n(t)$, Eq. (6), describes the output of a Wiener filter.[20]

We now show that the active processor, shown in Fig. 2, adaptively performs matched filtering. The exact input–output relationship is given by

$$\begin{aligned} e(t) &= \int_{-\infty}^{\infty} x(t-\tau) s^*(-\tau)\, d\tau \\ &\quad - G \iint_{-\infty}^{\infty} x(t-\tau) x^*(\alpha) e(\tau+\alpha)\, d\alpha\, d\sigma\, d\tau, \end{aligned} \tag{7}$$

where $e(t)$ is the output signal of the active processor. The assumption of low input SNR along with the conditions stated previously allows the following approximate form of Eq. (7):

$$\begin{aligned} e(t) &\approx \int_{-\infty}^{\infty} x(t-\tau) s^*(-\tau)\, d\tau \\ &\quad - G \iint_{-\infty}^{\infty} n(t-\tau) n^*(\alpha) e(\tau+\alpha)\, d\alpha\, d\sigma\, d\tau. \end{aligned} \tag{8}$$

Adaptive acoustooptic filter

Appendix A

Demetri Psaltis and John Hong

A new adaptive filter utilizing acoustooptic devices in a space integrating architecture is described. Two configurations are presented; one of them, suitable for signal estimation, is shown to approximate the Wiener filter, while the other, suitable for detection, is shown to approximate the matched filter.

I. Introduction

The design of optimum systems, in the classical sense, requires *a priori* some knowledge of the signals to be encountered. As a result, such systems perform poorly when the appropriate characteristics of the input signals are not known *a priori* sufficiently well or are time-varying. An adaptive processor has the ability to self-optimize by continually monitoring its performance and updating its parameters. Adaptive techniques have been applied to both spatial and temporal filtering domains. Specifically, adaptive techniques have been applied to antenna array processing by Appelbaum,[1] Widrow,[2] and others.[3,4] Applications to time domain problems include Lucky's work on data redundancy removal,[5] Sondhi's adaptive echo canceler,[6] Widrow's work on adaptive noise suppression,[7] Morgan and Craig's adaptive linear predictor,[8] and more.[9-11]

In the work on time domain problems cited above the adaptive filtering scheme is based on the orthogonality principle.[12] The basic idea behind the scheme is to control a variable filter so as to minimize the correlation between the input signal and the residual signal, which is the difference between the input signal and the filter output. A particular implementation of this scheme uses the transversal filter architecture, which consists of a tapped delay line, variable filter weights, and a summer that produces a weighted sum of delayed versions of the input signal as its output.

The linearity and parallel nature of the transversal filter arrangement, commonly called the correlation cancellation loop (CCL) system, make the optical implementation possible. The advantages of optical processors in terms of bandwidth and the large effective number of taps make such an implementation attractive. For example, acoustooptic devices (AODs), which can serve as optically tapped delay lines, are superior in terms of bandwidth to CCD implemented delay lines that are currently used in analog adaptive filters.[13,14] Several adaptive optical filter implementations have been previously proposed. Psaltis *et al.*[15,16] proposed use of an iterative electrooptic processor for adaptive spatial filtering of phased array antenna signals. Rhodes[17] described a system using acoustooptic and electrooptic modulators in a time integrating architecture to implement the CCL algorithm in the time domain, and VanderLugt[18] described an optical processor which is a frequency domain implementation of the CCL algorithm. Lee *et al.*[19] have devised an adaptive filter which suppresses narrowband interference from wideband signals using an acoustooptic spectrum analyzer with an array of electrooptic modulators in the spatial frequency plane which can adaptively excise strong narrowband components of the signal spectrum.

In this paper, we describe a new method for adaptive inverse filtering in the time domain. Two implementations are presented; the first, the passive processor, performs the inverse filtering operation, while the other, the active processor, is capable of performing adaptive matched filtering operations. Both processors are space integrating systems and do not require optically addressed, time integrating spatial light modulators. These architectures implement the CCL algorithm in the time domain and are structurally simpler than their frequency domain implemented counterparts. The implementations are strictly one dimensional, and thus it is possible to extend this concept to 2-D processing problems through the use of multichannel AODs.

The adaptive processors are discussed at the system level in Sec. II, and the optical implementations of the system blocks are described in Sec. III. The two optical configurations of the adaptive filters are described in Sec. IV.

II. Adaptive Estimation and Detection

The extraction of information from a signal corrupted by additive noise requires *a priori* knowledge of the properties of the desired signal and the noise. If the necessary information is known, the optimum linear filters can be designed to satisfy the specified performance criteria. The Wiener filter provides the minimum mean square error estimate of a signal in the

The authors are with California Institue of Technology, Department of Electrical Engineering, Pasadena, California 91125

Received 27 April 1984.
0003-6935/84/193475-07$02.00/0.

For example if K=10 and a=1, we require the number of distinguishable levels at the output to be at least 100 for R to be equal to 1. It is important to note, that the output levels must be sufficiently well defined so that the A/D converter can detect all of them with very low probability of error. DR_2 is much smaller than what is conventionally called "detector dynamic range". We estimate that it would require very sophisticated - engineering to obtain DR_2=100 and it does not appear that DR_2=1000 is practically feasible in the foreseeable future. We believe that the answer to obtaining a high accuracy optical processor that is suitable for implementation of direct algorithms for adaptive antenna arrays is not likely to come from a well engineered DMAC based system. It is more likely that algorithms and architectures can be found that utilize more efficiently the capabilities of optics and rely less on the use of sophisticated post detection electronics.

[1] RADC-TR-83-156, "Acoustooptic Adaptive Processing (AOAP)", by General Electric Co., Dec. 1983.

[2] RADC-TR-81-130, "Efficient Digital Algorithms for Adaptive Arrays", by Niel A. Carlson, 1981.

For comparison, consider the Fourier Transform of Eq.6; when the accumulation time is infinite, the optimum filter equation is given by

$$2\sum_{j=1}^{N}\Gamma_{ij}(\omega)H_j(\omega) = \lambda^{*}S_i^{*}(\omega), \qquad (12)$$

$$\Gamma_{ij}(\omega) = \text{F.T.}\ [\ \gamma_{ij}(\tau)\ ],$$

where $\Gamma_{ij}(\omega)$ is the spectral density matrix. Identifying the integral in Eq.11 as the smoothed estimate of the spectral density matrix of the input noise vector, Eq. 11 is approximately equivalent to Eq.12. The effect of the finite time integration window is seen in the smoothing of the noise spectrum.

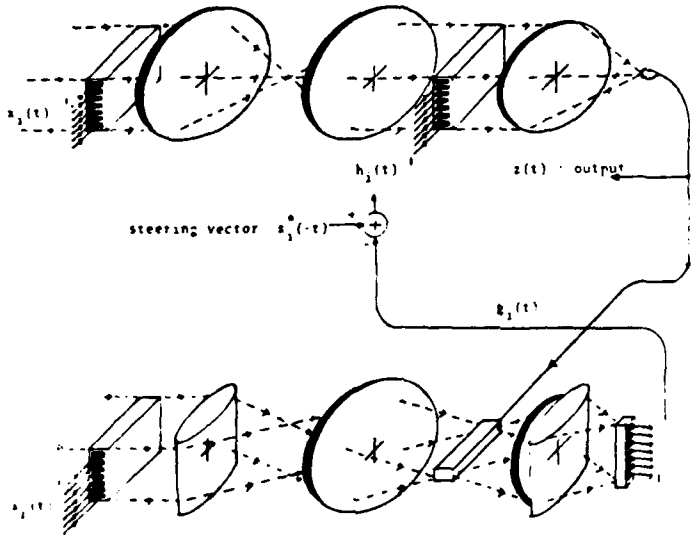

Fig.11 Adaptive Acoustooptic Phased Array Processor

Acknowledgement

This work is supported by the Rome Air Development Center and, in part, by the Air Force Office of Scientific Research.

IV. References

1. R. Riegler and R. Compton, Jr., 'An Adaptive Array for Interference Rejection, Proc.IEEE 61,748 (1973).

2. J. F. Rhodes,'Adaptive Filter with a Time-Domain Implementation Using Correlation Cancellation Loops,' Appl.Opt.22, 282 (1983).

3. A. Vanderlugt, 'Adaptive Optical Processor,' Appl.Opt.21, 4005 (1982).

4. D. Psaltis and J. Hong, 'Adaptive Acoustooptic Filter,' Appl.Opt.23, 3475 (1984).

Appendix C

Volume 52, number 3 OPTICS COMMUNICATIONS 1 December 1984

A SPACE INTEGRATING ACOUSTO-OPTIC MATRIX–MATRIX MULTIPLIER

Kelvin WAGNER and Demetri PSALTIS
Department of Electrical Engineering, California Institute of Technology, Pasadena, CA 91125, USA

Received 9 August 1984

An optical architecture is described for performing pipelined matrix–matrix multiplications. The architecture is implemented using multiple transducer acousto-optic devices and a wideband photodetector array. A variant of engagement formatting allows multiple inner products to be simultaneously computed by 1-D spatial integration, and through proper pipelining the full product matrix is produced at the output of the detector array. The output matrix in this architecture is in a format that is directly compatible with the input, a feature that can facilitate the implementation of iterative matrix algorithms. Digital multiplication by analog convolution can be incorporated for improved accuracy by using a frequency multiplexed representation of the binary data.

1. Introduction

The optical implementation of matrix operations has received considerable attention recently. Architectures and algorithms have been designed that have increased the speed, accuracy and flexibility of optical matrix processors, extending the potential applicability of such systems to a broader range of problems. Specific advances that have been accomplished in recent years include the initial demonstration of vector–matrix multiplication [1], the introduction of time integrating systolic [2], engagement [3,4], and outer product optical processors [5], a frequency multiplexed processor [6], improvements in accuracy with residue arithmetic [7], the utilization of the method of digital multiplication by analog convolution (DMAC) [8,9] in the above array processors [10,11], and a combination of systolic processing and the DMAC algorithm in a two dimensional implementation utilizing crossed multichannel Brag cells for matrix vector multiplications with digital accuracy [12].

Perhaps the most significant application of numerical optical processors is in $O(N_3)$ problems, i.e. matrix algebra problems that require a minimum of N^3 multiplications and additions, where N is the size of the matrix involved. The solution of a set of linear equations, matrix inversion, and singular value decomposition are examples of such problems [13]. Optical techniques can be applied to such problems by selecting an algorithm that can implement the required operation with successive matrix–matrix multiplications, such as Gauss eliminations, Givens transformations or Housholder reflections [13]. For these algorithms N optical matrix multiplications are required, and since each matrix–matrix multiplication requires N^3 multiplies and adds, optical systems usually solve an N^3 problem with N^4 operations. However, the speed and parallelism of optics can make the optical implementation advantageous, despite this inefficiency. The product matrix that is produced at each iteration during the execution of such an algorithm is used as one of the input matrices for the next iteration. It is therefore important that the format of the output product matrix is directly compatible with the input in order to avoid reformatting and minimize the iteration time. The architecture described in this paper was selected principally because the output can be amplified and applied directly to the input. A space integrating implementation using a parellel output wideband photodetector array is chosen for accuracy and speed considerations. Several candidate data flow optical architectures satisfying these requirements are possible. In this paper we present one such data flow matrix processor which uses crossed multichannel acousto-

0 030-4018/84/$03.00

optic devices (AOD). The operation of the system is based on time and space alignment of vectors which allows the formation of multiple inner product summations via spatial integration in a pipelined fashion. The matrix format is similar to an engagement array, but the data flow is transposed so that the local multiplications needed for each inner product operation form in parallel in space, rather than sequentially in time. Each inner product is summed by a 1-D space integrating condensing cylinder onto an output detector. Many such inner product accumulators are multiplexed in the orthogonal dimension onto separate detectors of a linear array.

2. Optical processor architecture

The proposed optical architecture for matrix–matrix multiplication is shown in fig. 1, along with the appropriate data flow. The principal components of the system are a pulsed laser, two orthogonal multichannel Bragg cells (one with N channels, and the other with $2N - 1$ channels), a linear array of N wideband photodetectors, and lenses. The optical processor is a 2-D array of N^2 analog multipliers configured as an array of N space integrating inner product processors. With the appropriate engagement format of the matrices an array of inner products is formed on the detector array during each processor cycle. As data flows through the Bragg cells the output appears in the same engagement format as the input, which allows direct feedback for iterative operations without latency.

Global system synchronization and sample definition at the output are provided at each time interval T, by the strobing action of a repetitively pulsed laser diode. The pulsed light is collimated and incident on the first multichannel acousto-optic device, AOD1, at the Bragg angle in the x dimension. The elements of an $N \times N$ matrix A are applied to the N transducers of AOD1 in an engagement representation. They propagate continuously along the x direction at a velocity equal to one inter transducer spacing of AOD2 each T s. Rows are represented in individual channels as sequential acoustic pulses separated by T s. The nth row of the matrix A is applied to the nth transducer of AOD1 with a delay of nT s. In this manner the matrix is folded back in time into a sliding parallelogram format we call time engagement. The optical field emerging from AOD1 is spatially filtered in the Fourier plane to remove the undiffracted component and the diffracted field is imaged onto AOD2 at the Bragg angle in y. For clarity the image reversal of the imaging system is ignored. Matrix B propagates in AOD2 in the y direction one channel separation of AOD1

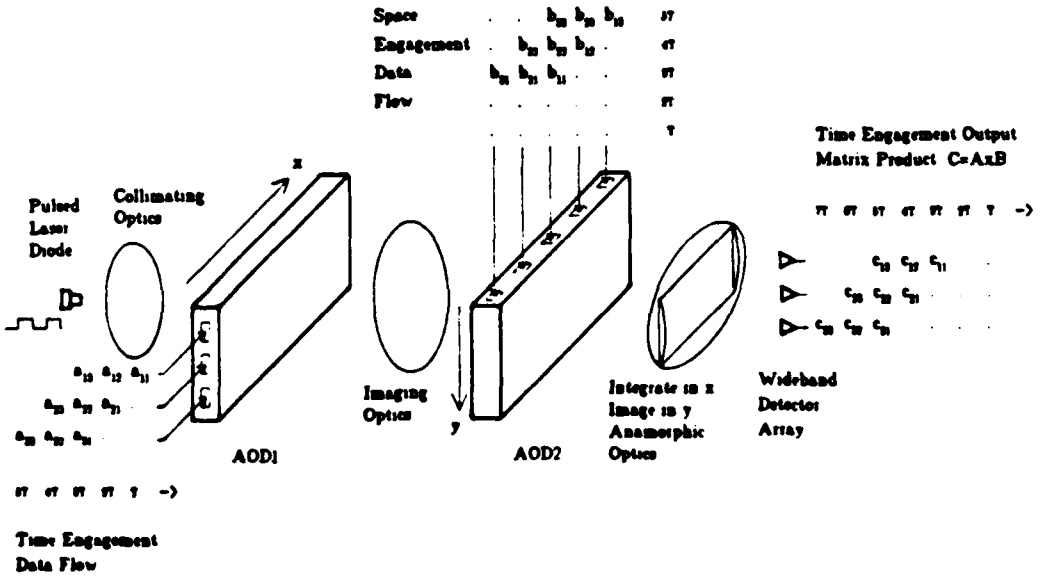

Fig. 1. Schematic representation of the space integrating acousto-optic matrix–matrix multiplier, with the associated engagement data flow. (For simplicity, the details of spatial filtering and the effect of image reversal are neglected in this figure.)

each T s, orthogonally to, and synchronously with, the motion of A. B is delayed by $(N-1)T$ s with respect to A to allow the first row of A to fully enter AOD1. At time $(N-1+k)T$, the kth column of the matrix B is applied to transducers k through $k+N$ of AOD2. In this representation, called space engagement, the matrix is folded over in space to $2N-1$ parallel channels which require N time cycles to be completed. The doubly diffracted light is imaged in y and space integrated in x by the anamorphic lens system following AOD2. The light collected on each photodetector during each cycle is the sum of the product of the elements that are aligned within the corresponding horizontal channels of the two AODs. As we will see in the following paragraph, at the output of the detector array we obtain the product matrix $C = A \times B$ in a time engagement format.

At the Nth time increment the first row of matrix A in AOD1 and the first column of matrix B in AOD2 are spatially aligned in the top channel of the system. The N local products $a_{1i}b_{i1}$ are calculated in parallel by imaging AOD1 through AOD2, and the sum $c_{11} = \Sigma_{i=1}^{N} a_{1i}b_{i1}$ is produced by spatially integrating all these products onto the top detector. One time increment T later the second row of A has fully entered the second channel of AOD1, and simultaneously the first row of A has moved one column away from the transducer. In the orthogonal dimension, the first column of B has moved down in AOD2 one channel to engage the second row of A and produce $c_{21} = \Sigma_{i=1}^{N} a_{2i}b_{i1}$ via space integration onto the second detector. Concurrently the second column of B has been applied to transducers 2 through $N+1$, in order to align with the first row of A and produce $c_{12} = \Sigma_{i=1}^{N} a_{1i}b_{i2}$ on the first detector. In a similar manner successive inner products are aligned, locally multiplied and globally accumulated to the N output detectors. In a total of $2N-1$ time increments T, the output product matrix is produced in a time engagement format identical to the format of the matrix A. Therefore it can be fed directly back to the N transducers of AOD1 with no reformatting or latency. This allows for fully efficient pipelining of iterative matrix algorithms, since after the matrix A is initially loaded into AOD1 there are no more waiting periods required to load new matrices. For instance, when the first element of the output matrix c_{11} is produced the first row of A has been fully entered into OAD1 so we can begin entering the first row of the output matrix in the top channel of AOD1. No interference with subsequent calculations will occur because of the zeroes included in the space engagement formatting of matrix B.

If the Bragg cells are operated in the linear amplitude diffraction regime, and coherent detection is used, then it is possible to make the outputs of the photodetectors appear at the center frequency of AOD1, simplifying direct feedback. The coherent implementation allows complex valued matrices to be represented by the magnitude and phase of the acoustic pulses. If the Bragg cells are operated in the linear intensity diffraction regime (incoherent implementation), then only real positive matrices can be represented, but simpler non-interferometric detection can be employed. In this case the output matrix would not be on a carrier, therefore mixers would be required to upconvert the output before amplifying and applying to AOD1.

3. Frequency multiplexed DMAC

An increase in the accuracy of this processor can be incorporated by the use of the digital multiplication by analog convolution algorithm (DMAC) [8–12], at the expense of additional complexity. It is well known that the multiplication of two time domain waveforms results in the convolution of their Fourier spectra. This can be utilized to implement the DMAC algorithm by simply multiplying the frequency multiplexed binary representations of two numbers.

The product $z = x * y$ of two M bit integers x and y can be expressed as follows:

$$z = \sum_{k=0}^{2(M-1)} z_k 2^k = \left(\sum_{i=0}^{M-1} x_i 2^i\right)\left(\sum_{j=0}^{M-1} y_j 2^j\right)$$

$$= \sum_{k=0}^{2(M-1)} 2^k \left(\sum_{i=0}^{M-1} x_i y_{k-i}\right), \qquad (1)$$

where x_i, y_i are the bits in the binary representation of the integers x and y and the coefficients $z_k = \Sigma_{k=0}^{M-1} x_i y_{k-i}$ can achieve M discrete levels. A time domain representation of a frequency multiplexed binary word is given by $f(t) = \Sigma_{n=0}^{M-1} x_n \exp(jn\omega t)$. The product of two such waveforms is

$$h(t) = f(t)\,g(t)$$

$$= \left(\sum_{n=0}^{M-1} x_n \exp(jnwt)\right)\left(\sum_{m=0}^{M-1} y_m \exp(jmwt)\right)$$

$$= \sum_{k=0}^{2(M-1)} \left(\sum_{n=0}^{M-1} x_n y_{k-n}\right) \exp(jkwt)$$

$$= \sum_{k=0}^{2(M-1)} z_k \exp(jkwt). \qquad (2)$$

Thus the weights of the frequency multiplexed product waveform correspond to an M level digitally weighted representation of the product of the two binary words. This pseudo binary representation can be channelized into $2M-1$ frequency channels, each centered at kw. The amplitude of each spectral component can be quantized to one of M levels by an A/D converter, and true binary representation can be obtained with a digital shift and add register.

Digital multiplication by frequency convolution can be incorporated in the matrix multiplier of fig. 1 in order to improve the accuracy over that attainable with analog data representation. This will increase the required time bandwidth product of the AODs by a factor of at least the number of bits. The duration of the optical and acoustic pulses must be at least $2\pi/w$ s, to permit channelization at the detector output. The frequency multiplexed binary weighted data must be encoded in phase within each acoustic pulse so that all the frequency components add constructively. When interferometric detection is used, the RF output from each detector will be the coherent sum of N frequency multiplexed multilevel binary weighted signals, occupying up to twice the original bandwidth. This format is compatible with direct feedback to AOD1 without redigitization in each cycle. Further iterations would increase the required dynamic range of each frequency component and increase the number of nonzero frequencies. By examining the Fourier plane of AOD1 we can determine globally the number of frequencies occupied for matrix A. If the available number of frequency bins is exceeded by p excess Fourier components, then we can perform a global pseudo floating point rescaling of the product matrix by increasing the local oscillator frequency used for heterodyne detection by pw. The lower order p bits are then discarded by highpass filtering the detector outputs, or with a Fourier plane aperture. Redigitization is required if a detectors dynamic range is exceeded or when the iterative matrix operation has converged, and the resultant matrix must be output in binary form.

The major difficulty with incorporating DMAC in the matrix–matrix multiplier is the complexity of the frequency multiplexed encoding and decoding, and the large number of A/D converters required to convert back to true binary form. Each of the N detectors must be channelized into $2M$ frequency bands, and each of these must be digitized every T s to an accuracy of NM. This could require as many as $2NM$ A/Ds, which is probably impractical. Alternatively, N faster A/Ds could be multiplexed between $2M$ frequency channels each by performing a conversion each $T/2M$ s. To decrease the number of A/Ds even further it may be possible to digitize only one detector output at a time, and recycle the matrix for further conversions by multiplying by the identity matrix I.

4. Discussion

Acousto-optic devices are attractive transducers for data flow optical processors because of their sliding window nature, wide bandwidth (>1GHz), large number of resolvable spots (TB>1000) and wide dynamic range (>60dB). When dealing with multichannel Bragg cells, however, the constraints imposed by acoustic diffraction and electrical crosstalk limit all aspects of device performance. Today a practical limit on the number of channels is on the order of 100 or less. Eventually larger arrays may be realized through the use of anisotropic self collimation and effective RF isolation techniques. The properties of the multichannel acousto-optic devices determine the processing power of the matrix multiplier and to a lesser degree the accuracy obtainable. In order to perform an $N \times N$ analog matrix multiplication this architecture would require an N channel AOD with TB = $2(2N-1)$ (AOD1), and a $2N-1$ channel AOD with TB = $2N$ (AOD2), where a factor of 2 was included for intra pulse dead time. If frequency multiplexed binary encoding is used with M bits, then AOD1 requires a TB > $M(2N-1)$, and AOD2 requires a TB > NM.

The detector array is composed of N parallel wideband photo-detectors whose outputs are bandpass filtered, combined with a steering matrix, amplified, and fed back to AOD1. Single photodetectors can have a wide dynamic range (>50dB), but large monolithically

fabricated arrays are limited by crosstalk. To obtain the full dynamic range capabilities of the detectors, a powerful optical source must be employed, and optical losses minimized.

To obtain an estimate of the processing power of the space integrating optical matrix multiplier described in this letter, let us consider a target system for multiplying 32 X 32 matrices. AOD1 requires 32 channels and a TB > 128, OAD2 requires 63 channels and a TB > 64. If we assume a bandwidth of 128 MHz, then the full matrix product could be obtained in 1 μs, yielding an analog processing rate of 3.2×10^{10} multiplications per second. At these rates the matrix could be inverted in as little as 32 μs with a direct algorithm, or a fraction of a millisecond with an iterative algorithm. If we desire digital accuracy of 8 bits input and 16 bits output, then the system parameters become much more stringent. AOD1 requires a TB > 1024, and AOD2 requires a TB > 512, which could be accomplished with a bandwidth of 100 MHz, and a matrix multiplication time of approximately 10 μs. This yields a processing rate of 3×10^9 DMAC multiplications per second. However, to obtain this additional accuracy we require an array of 32 frequency channelizers with 16 frequency bins each, and 32 8-bit A/D operating at 100 MHz, temporally multiplexed between the frequency channels. When the complexity of the electronic peripherals to the optical processor reaches this high level, it is important to keep in perspective what would be required for a fully digital implementation. For instance, for the same numbers as above a digital array of 32 8-bit multipliers/accumulators each operating at 100 MHz can have the same processing power (3.2×10^9 operations/s). In other words, comparable electronic hardware is needed for both the digital and the DMAC optical implementations. The advantage of the optical implementation is in the reduced communication rate (320×10^6 samples/s versus 3.2×10^9 samples/s in this example) between the high speed array processor and the system buffer memory. This advantage derives from the 2-D parallelism of optics which results in 1024 parallel multiplications being performed each 100 ns interval.

5. Conclusion

A highly parallel, pipelined, space integrating, acousto-optic processor for iterative matrix–matrix multiplication has been described. The architecture avoids the serial readout bottleneck and dynamic range limitations of CCD arrays used in time integrating architectures. The wideband nature of the input and output transducers can result in an analog processing rate exceeding 30 GOPs (Billion multiplies per second), and in excess of 3 GOPs for the DMAC implementation. Additional accuracy can be incorporated by the use of the DMAC algorithm and frequency multiplexing, but the improved accuracy is accompanied by an increase in complexity and expense. The analog optical processor can be implemented with currently available devices and simple electronic support circuitry. It provides extremely high processing power with reasonably good accuracy (equivalent to 8–10 bits) due to the high dynamic range that is achievable with non integrating photodiode arrays.

Acknowledgements

The research reported here is supported by the Air Force Office of Scientific Research and the Rome Air Development Center. K. Wagner is the recipient of an Army Research Office graduate fellowship. Illuminating discussions with T. Weverka and E. Miles are gratefully acknowledged.

References

[1] J.W. Goodman, A.R. Dias and L.M. Woody, Optics Lett. 2 (1978) 1.
[2] H.J. Caulfield, W.T. Rhodes, M.J. Foster and S. Horvitz, Optics Comm. 40 (1982) 86.
[3] P.S. Guilfoyle, Proc. SPIE 352 (1982) 2.
[4] R.P. Bocker, Appl. Optics 22 (1983) 804.
[5] R.A. Athale and W.C. Collins, Appl. Optics 21 (1982) 2089.
[6] D. Casasent, J. Jackson and C. Neuman, Appl. Optics 22 (1983) 115.
[7] J. Jackson and D. Casasent, Appl. Optics 22 (1983) 2817.
[8] H.J. Whitehouse and J.M. Speiser, in: Aspects of signal processing, pt 2, ed. G. Tacconi (Proc. NATO Advanced Study Institute) Boston (1976) pp. 669–702.
[9] D. Psaltis, D. Casasent, D. Neff and M. Carlotto, Proc. SPIE 232 (1980) 151.
[10] R.P. Bocker, S.R. Clayton and K. Bromley, Appl. Optics 22 (1983) 2019.
[11] R.A. Athale, W.C. Collins and P.D. Stilwell, Appl. Optics 22 (1983) 368.
[12] P.S. Guilfoyle, Opt. Eng. 23 (1984) 20.
[13] G.H. Golub and C.F. VanLoan, Matrix computations (John Hopkins University Press, Baltimore, 1983).

END

FILMED

9-85

DTIC